Hindawi
Geofluids
Volume 2022, Article ID 5637971, 15 pages
https://doi.org/10.1155/2022/5637971

Research Article

Data-Driven Methodology for the Prediction of Fluid Flow in Ultrasonic Production Logging Data Processing

Hongwei Song,[1,2] **Ming Li**,[3] **Chaoquan Wu**,[3] **Qingchuan Wang**,[3] **Shunke Wei**,[3] **Mingxing Wang**,[1] **and Wenhui Ma**[3]

[1]*College of Geophysics and Petroleum Resources, Yangtze University, Wuhan, Hubei 430100, China*
[2]*Research Office of Yangtze University, Key Laboratory of Well Logging, China National Petroleum Corporation, Wuhan, Hubei 430010, China*
[3]*China National Petroleum Corporation, Beijing 100000, China*

Correspondence should be addressed to Hongwei Song; shw98wj@yangtzeu.edu.cn

Received 4 January 2022; Revised 12 February 2022; Accepted 3 March 2022; Published 15 March 2022

Academic Editor: Zhenzhen Wang

A new method for the determination of oil and water flow rates in vertical upward oil-water two-phase pipe flows has been proposed. This method consists of an application of machine learning techniques on the probability density function (PDF) and the power spectral density (PSD) of the power spectrum output of an ultrasonic Doppler sensor in the pipe. The power spectrum characteristic parameters of the two-phase flow are first determined by the probability density function (PDF) method. Then, the transducer signal is preprocessed by distance correlation analysis (DCA), and independent features are extracted by principal component analysis (PCA). The extracted features are used as input to a least-squares fit, which gave the oil flow rates as output. In the same way, the transducer signal is also preprocessed by partial correlation analysis (PCA), and independent features were extracted using independent component analysis (ICA). The extracted features were used as inputs to multilayer back-propagation neural networks, which water cuts as output. The present method was used to calibrate an ultrasonic Doppler sensor to estimate the flow rates of both phases in oil–water flow in a vertical pipe of diameter 159 mm. Predictions of the present method were in good agreement with direct flow rate measurements. Compared to previously used methods of feature extraction from the ultrasonic Doppler power spectrum signals, the present method provides a theoretical basis for the interpretation of ultrasonic multiphase flow logging data. Ultrasonic multiphase flow logging has potential application value in the production profile logging and interpretation evaluation of production wells with low fluid production and high water cut.

1. Introduction

Production logging is a major means of oil well dynamic monitoring. It is an important issue in the logging industry to understand the production status of the oil well production layer, the remaining oil production of the reservoir, the evaluation of the reservoir reconstruction effect, and the adjustment and improvement of the development plan [1]. The production logging technology also plays a very important role in the development of oil fields.

However, oil fields with low porosity and low permeability in the middle-late mining stage are characterized by low flow rate, high water cut, and sand out. The oil-water two-phase flow in the oil well has complex flow regimes with random and variable oil-water interface, as well as a serious slip effect between the oil and water phases. These problems have caused major challenges to traditional production profile logging, such as spinner flowmeter responds poorly under low flow conditions, and the fluid capacitance has poor response under high water cut conditions [2]. Ultrasonic multiphase flow logging tool is a logging method that uses the ultrasonic Doppler effect and the difference in acoustic impedance between oil, gas, and water and uses the spectral characteristics of the discrete phase reflected sound waves to obtain the flow of fluids in each phase [3]. Ultrasonic multiphase flow logging technology solves the

problems of two-phase flow and three-phase flow logging in complex well conditions (low production fluid, sand out, highly deviated well, etc.), and the logging data provides a reliable basis for oilfield development engineers [4]. At this stage, the realization of the instrument method is relatively mature, and the difficulty lies in how to extract information that can accurately reflect the flow of oil, gas, and water from a single ultrasonic frequency spectrum data [5].

Due to the nonlinearity of the data, there are many difficulties in establishing an accurate prediction model. The measurement precision of split-phase flow is lower. Therefore, it is significant to study on the soft measurement method of split-phase flow. In recent years, machine learning models have begun to be applied in various fields. Several investigators suggested the artificial neural network (ANN) methods to solve this problem for multiphase flow [6–8]. ANN techniques have been proposed as a powerful and computational tool to model and solve the complex problems that cannot be described with simple mathematical models [9–11]. Osman presented an ANN model for prediction of pressure drop in horizontal and near-horizontal gas–liquid flow [12]. Zhao et al. established an ANN prediction model based on the conductance signal obtained by measuring the oil-water two-phase flow with electrical methods, where water cut was from 51% to 91%, and good prediction results were obtained [13].

Dimensionality reduction methods are an essential step in any machine learning model pipeline since they will have major importance regarding the accuracy of the classification or regression algorithm applied to the data [14]. Principal component analysis (PCA) is the most commonly used dimensionality reduction method. PCA was originally introduced by Pearson [15] and developed independently by Hotelling [16]. PCA is an unsupervised linear mapping based on an eigenvector search and suitable for Gaussian data. PCA provides different strategies for reducing the dimensionality of feature space and preserves the maximum amount of variance of the original data [17, 18]. PCA can be computed using different algorithms including eigenvalues, latent variable analysis, factor analysis, or linear regression (LR) [19]. Major applications of PCA include image and speech processing, visualization, exploratory data analysis, and robotic sensor data [20].

Aiming at the oil-water two-phase production characteristics of low production, high water cut, and obvious slippage, in order to improve the interpretation accuracy and dig out more ultrasonic multiphase flow logging information, this paper carried out the oil-water two-phase simulation logging experiment of the ultrasonic multiphase flow logging tool to study the ultrasonic frequency spectrum information of the oil-water two-phase flow and the oil and water flow interpretation model. It provides a new interpretation method for the ultrasonic multiphase flow logging of oil-water two-phase production wells with low production liquids.

2. Experimental Facility and Logging Tool

All logging experiments were conducted in the oil-water flow facility at the Yangtze University in China (Figure 1), and the ultrasonic multiphase abortion profile production logging instrument is shown in Figure 2.

This facility was mainly composed of clear Perspex tubing with an inner diameter of 159 mm, which permitted visual observation of the flow, and the wellbore angle is vertical 90° (relative to the ground). The water of the experimental medium is tap water (density 988 kg/m^3, viscosity 1.16 mPa·s), and the oil is 10# industrial white oil (density 826 kg/m^3, viscosity 8.29 mPa·s). The total flow rate (Q_m) in the experiment ranges from 0.5 m^3/d to 40 m^3/d; the water cut (C_w) varies from 0% to 100%. The oil and water are transported by peristaltic pumps to the pressure-stabilized irrigation and then enter the metering pipeline to ensure that the fluid flow in the oil-water transportation pipeline can ignore the impact of the pump pulsation. The oil and water volumetric flow rates were controlled by butterfly valves, and they were measured by high-precision mass flowmeter (KLB-CMFI-DN6). A total of 42 sets of experimental operating conditions for oil-water two-phase flow with different total flow rates and different water cuts were designed for the experiment. In order to ensure that the fluid flow is sufficiently stable, the measurement of the ultrasonic logging instrument probe was set at 6.0 meters from the inlet of flow fluid; after the oil-water flow rate of each experimental point stabilized for 30 minutes, the ultrasonic instrument started the test and continued at least 3 pulse periods, and the test scenario is shown in Figure 3. All experiments were conducted normal temperature and under the atmospheric pressure.

The structure of the ultrasonic multiphase flowmeter is shown in Figure 2. The ultrasonic probe is located at the lower end of the instrument string during well logging, and the instrument string is connected to the centralizer to make the instrument centered for measurement. The ultrasonic probe adopts spontaneous and self-receiving measurement, and the transmitting and receiving surfaces are conical [4]. Basic principle is the ultrasonic probe that is the transmission of ultrasonic signal by cone, and sound waves meet continuous water phase in the discrete phase (oil bubble, bubble) reflects, when the ultrasonic wave propagation direction and oil bubble movement direction are 90°, ultrasonic reflection in oil bubble surface, and the frequency of the reflected ultrasonic wave relative to change in the frequency of the ultrasonic before reflection, this change is the Doppler frequency shift.

Transducer T emits ultrasonic waves of frequency f_0 to the fluid, and transducer R receives the waves scattered by a particle in the sample volume [21]. Owing to the relative motion between the particle and transducer T, the frequency f_1 of incident waves received by the particle is modulated according to the Doppler effect:

$$f_1 = \frac{c + u\cos\theta}{c} f_0, \tag{1}$$

where c is the speed of sound in fluid, u is the particle velocity in the main flow direction, and θ is the angle (Doppler angle) between the sound beam axis and particle flow direction. For the scattering waves, the moving particle is considered a

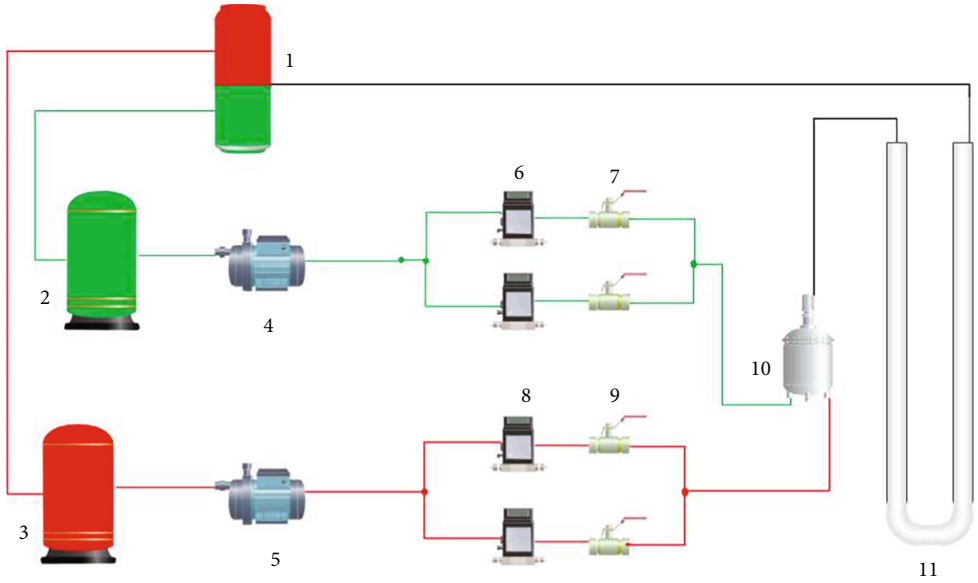

1. Oil-water separation tank; 2. Water piggy tank; 3. Oil piggy bank; 4. Water pump; 5. Oil pump; 6 Mass flowmeter; 7. Waterway control valve; 8. Mass flowmeter; 9. Oilway control valve; 10. Oil-water mixer; 11. Simulated wellbore;

Figure 1: Schematic diagram of multiphase flow simulation well experiment device.

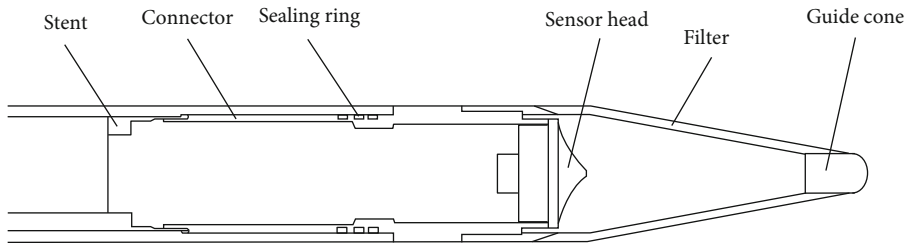

Figure 2: Schematic diagram of ultrasonic multiphase flow logging tool structure.

Figure 3: Simulation logging experiment diagram.

secondary ultrasound source, and the relative motion between the particle and transducer R produces a second Doppler effect. Hence, the frequency f_r of scattering waves received by transducer R is also modulated by the relative motion between it and the particle, which can be expressed as

$$f_r = \frac{c}{c - u\cos\theta} f_1 = \left(1 + \frac{2u\cos\theta}{c - u\cos\theta}\right) f_0. \tag{2}$$

Because the flow velocity u is usually much lower than c, the term $(c - u\cos\theta)$ in Eq. (2) can be approximated as c, which simplifies frequency f_r to

$$f_r \approx \left(1 + \frac{2u\cos\theta}{c}\right) f_0. \tag{3}$$

As a result, the Doppler shift of a single oil bubble can be calculated from [22]

$$f_d = f_r - f_0 = \frac{2u\cos\theta}{c} f_0. \tag{4}$$

The signal reflected by a large number of oil bubbles in the wellbore and the acoustic signal of the wellbore straight lotus are superimposed on the receiving transducer. The signal is transmitted and amplified by telemetry. The final difference frequency signal obtained is the Doppler signal of the ultrasonic multiphase flowmeter [23]. The amount of frequency change is related to the movement speed of the oil bubble, and the amount of reflection of the ultrasonic wave on the surface of the oil bubble corresponds to the number of oil bubbles. Ultrasonic multiphase flow meters use the Doppler frequency domain effect of reflected and scattered ultrasonic signals to obtain fluid flow information [24].

The center frequency of the probe is set to 750 KHz, the measurement method adopts the static point measurement of the instrument, the test time of each experimental measurement point is 3 minutes, and at least 3 cycles of data are collected. The probe is at the foremost end of the instrument string, the fluid is in a noncollecting condition, and the state of the fluid to be measured is basically unchanged. When it flows through the ultrasonic probe, measurement is performed to collect data.

3. Analysis of Experimental Results

3.1. Characteristics and Spectrum Analysis of Instruments Influencing Oil-Water Two-Phase Flow. In order to study the response characteristics of the ultrasonic flowmeter to the oil bubble flow, the logging data collected by the ultrasonic flowmeter was analyzed and processed by the power spectrum, the hydrostatic oil injection (the wellbore is filled with water, increasing the flow of oil), and power spectrum curve (as shown in Figure 4). The power spectrum curve of the same total flow and different water cuts is as the oil-water two-phase flow (as shown in Figure 5). From Figures 4 and 5, the flow characteristics of the fluid at the measuring point can be qualitatively analyzed by the curve change trend.

In the case of hydrostatic oil injection, the amplitude of the power spectrum curve increases with the increase of oil flow. The greater the oil flow, the stronger the reflected signal. When the oil flow rate is very low (less than 1.5 m^3/d), most of the acoustic waves emitted by the ultrasonic sensor are dispersed, the reflected waves are weak, the amplitude is low, and the measurement effect is not obvious. With the increase of oil flow, discrete oil bubbles in the continuous water phase increase, and part of the sound wave is reflected on the surface of the oil bubble. The amplitude of the reflected sound wave is relative to the number of oil bubbles. The more oil bubbles (the larger the oil holdup), the stronger the reflected wave, and the larger the amplitude. Because the water is still, the oil bubbles move upwards at a static drift speed in the water, and the slip phenomenon is obvious [25]; so, the relationship between the change of the center frequency and the change of the oil phase flow rate is not obvious. When the oil flow rate is greater than 20 m^3/d, the oil flow rate increases, but the center frequency decreases. That is, under low flow conditions, the increase in oil flow is mainly due to the increase in the number of oil bubbles (increased oil holdup), and the speed of oil bubbles hardly increases or even decreases. Therefore, in the case of low flow, especially when the water is static or the flow is very low, the center frequency has little correlation with the oil flow.

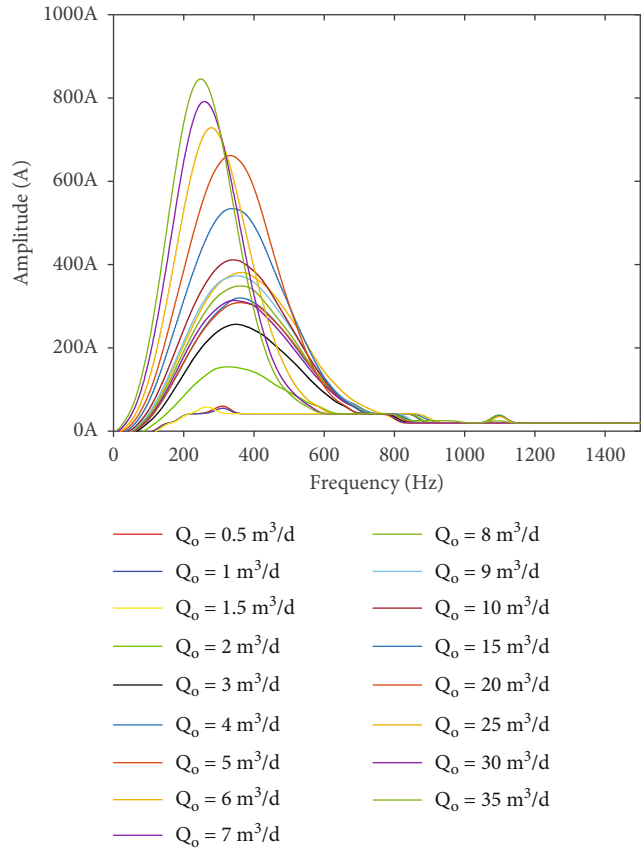

Figure 4: Hydrostatic oil injection power spectrum diagram.

In the case of oil-water two-phase flow, the amplitude of power spectrum curve, left and right attenuation coefficient, and center frequency has obvious changes under the same total flow and different water cuts. The center frequency moved to the right with the increase of water cut, and the peak amplitude decreased with the increase of water cut. This is mainly due to the increase in water cut and the decrease in oil flow. There are fewer discrete oil bubbles in the continuous water phase. Part of the sound waves reflects weakly on the surface of the oil bubbles, and the reflected wave received by the probe decreases, resulting in a drop-in amplitude peaks. The amplitude peak value and center frequency are proportional to the flow rate, but their proportional relationship is uncertain under different total flow well conditions. Therefore, it is necessary to use the statistical results of the power spectrum data measured by the experiment to find the relationship between the amplitude, frequency, and the oil and water flow and obtain the corresponding calculation model or make the relationship chart.

3.2. Measurement of Oil Flow Rates and Description of the Algorithm. For the flow rate prediction, the PDF and PSD are first calculated from the input signal, and appropriate features are extracted by using PCA. The preprocessing steps

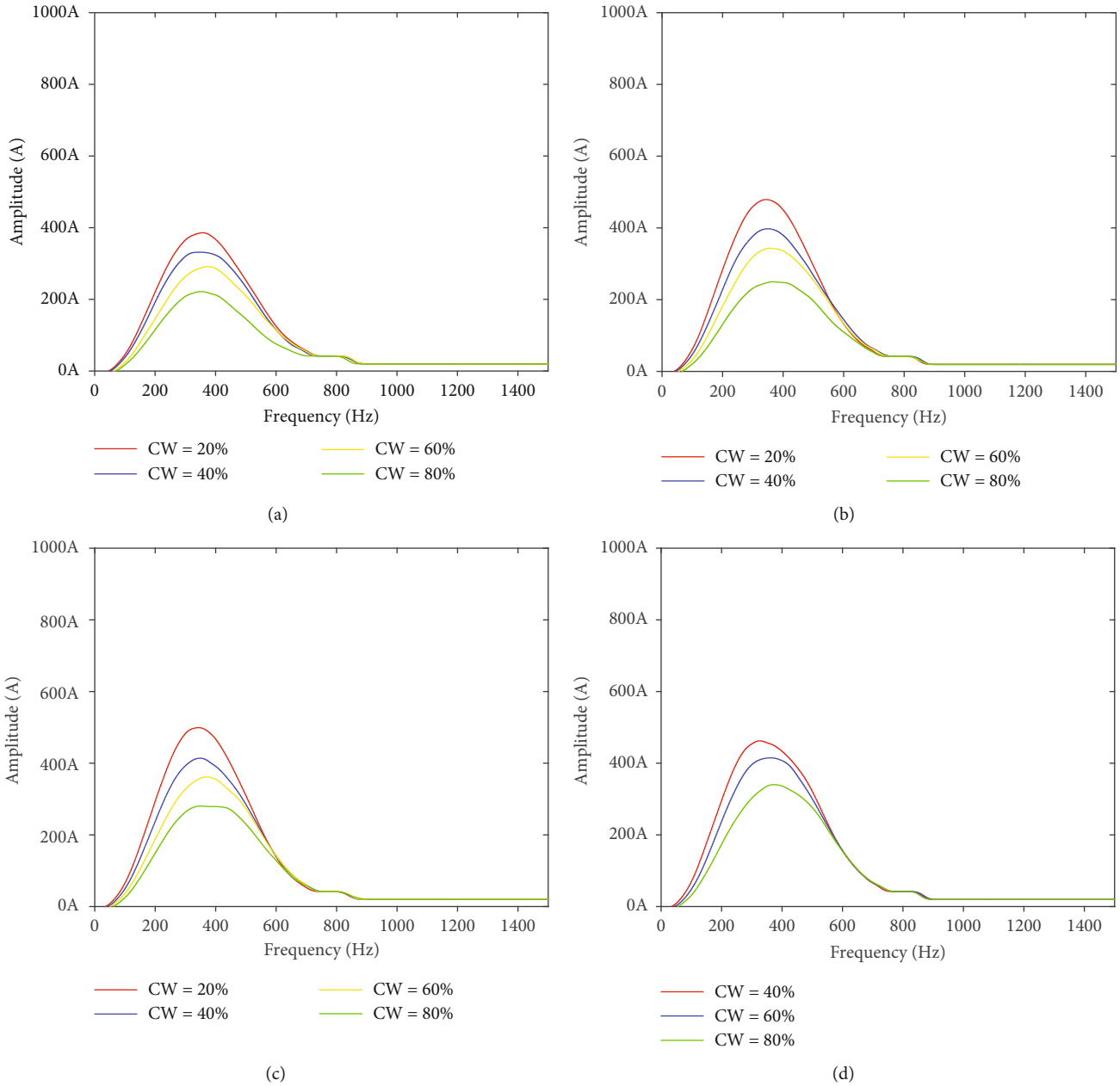

Figure 5: Continued.

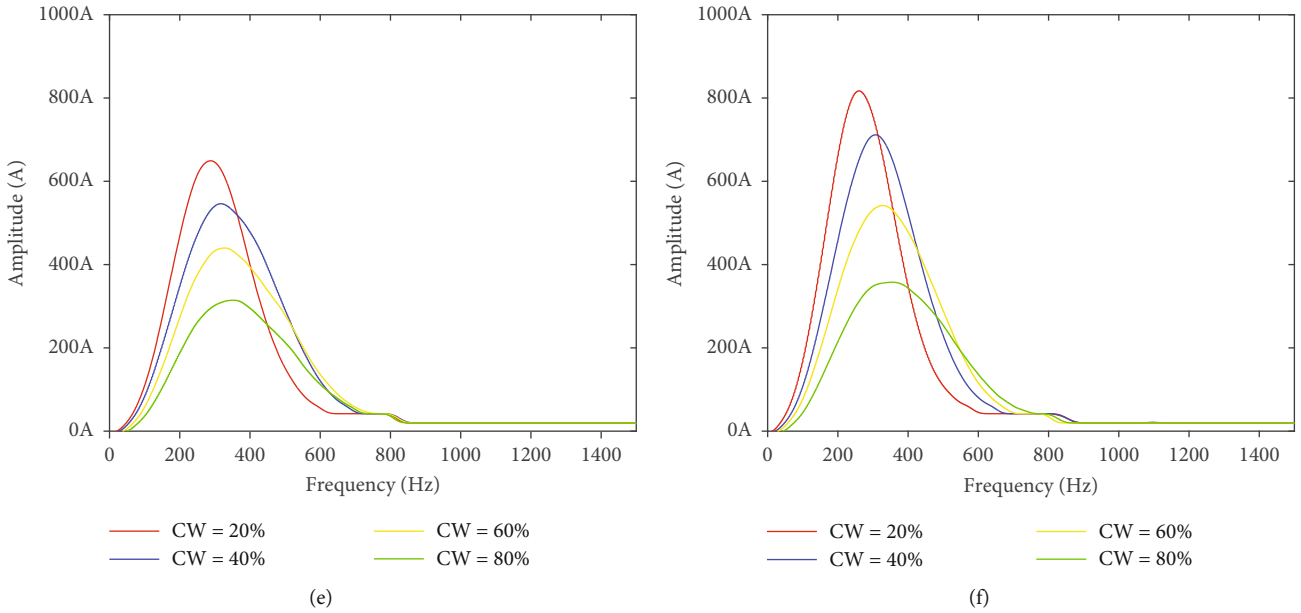

Figure 5: Power spectrum curve of oil-water two-phase flow: (a) Qm = 10 m^3/d, (b) Qm = 15 m^3/d, (c) Qm = 20 m^3/d, (d) Qm = 25 m^3/d, (e) Qm = 30 m^3/d, and (f) Qm = 40 m^3/d.

Table 1: Matrix table of approximate values of variables related to hydrostatic oil injection.

	Correlation between vectors of power spectrum							
	Oil flow	Peak amplitude	Center frequency	Amplitude of oil	Frequency of oil	Variance of oil	Area of oil peak	Logarithm of amplitude ratio
Oil flow	1.000	.960	-.610	.958	-.582	.048	.857	.787
Peak amplitude	.960	1.000	-.385	1.000	-.354	.294	.962	.920
Center frequency	-.610	-.385	1.000	-.377	.984	.693	-.140	-.029
Amplitude of oil	.958	1.000	-.377	1.000	-.348	.299	.966	.922
Frequency of oil	-.582	-.354	.984	-.348	1.000	.763	-.116	.024
Variance of oil	.048	.294	.693	.299	.763	1.000	.497	.641
Area of oil peak	.857	.962	-.140	.966	-.116	.497	1.000	.973
Logarithm of amplitude ratio	.787	.920	-.029	.922	.024	.641	.973	1.000

Table 2: Results of PCA.

Component	Eigenvalue	Variance contribution rate/%	Cumulative variance contribution rate/%
1	6.026	86.087	86.087
2	0.773	11.038	97.125
3	0.168	2.397	99.522
4	0.024	0.340	99.862
5	0.006	0.084	99.946
6	0.004	0.050	99.996
7	0.000	0.004	100.000

employ methods that preserve as much of the information contained in the differential the characteristic parameters as possible, albeit extracting features with a relatively small dimension.

In order to mine more power spectrum signal connotation, the one-dimensional probability density function (PDF) was used to fit the original measurement curve, and the characteristic parameters such as amplitude of oil, frequency of oil, variance of oil, and peak area of reaction oil bubble distribution and flow velocity information were obtained [26]. In order to reduce the complexity of the problem, the correlation analysis method is used to analyze the distribution parameters of the oil-water two-phase flow experiment and the characteristic parameters of the ultrasonic power spectrum to find the relationship between the characteristic parameters of the ultrasonic power spectrum and the oil-water flow parameters.

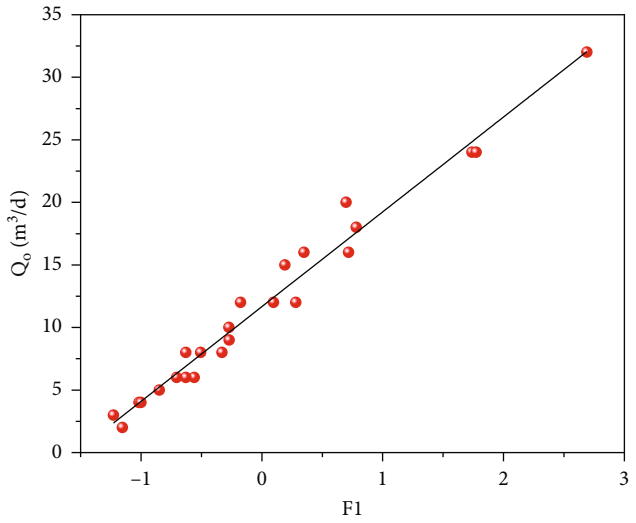

Figure 6: Diagram of relationship between Qo and F1.

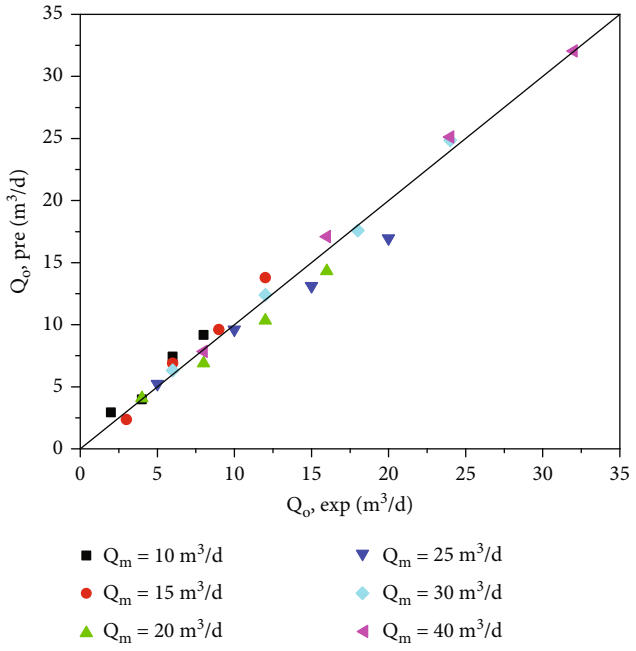

Figure 7: Forecast results of oil flow in oil-water two-phase flow.

First, the correlation analysis of the experimental rationing parameters of hydrostatic oil injection and the characteristic parameters of the ultrasonic power spectrum are carried out. The correlation analysis of the variables related to hydrostatic oil injection is based on the distance process correlation analysis. The approximate value matrix is shown in Table 1. The strength of the distance relationship between variables can be observed through the approximate matrix [27]. The results of the correlation analysis show that the oil flow has a good correlation with many characteristic parameters, if only one or two parameters for the traditional linear or nonlinear fitting to obtain the formula to calculate the oil flow, the results obtained error is larger, but too many variables will inevitably exist data duplication and superposition, resulting in the complexity of the algorithm to enhance. The basic principle of principal component analysis (PCA) is to integrate the original variables into several principal components, replacing a large number of variables with fewer combined variables, to minimize the loss of information carried by the variables, and to make them uncorrelated with each other [28]. The mathematical model of principal component analysis is as follows.

Suppose there are n samples, and each sample has p variables: $x_1, x_2, \ldots, x_p$, the original data observation matrix is as follows:

$$X_{n\times p} = \begin{bmatrix} x_{11} & x_{12} & \cdots & x_{1p} \\ x_{21} & x_{22} & \cdots & x_{2p} \\ \vdots & \vdots & \ddots & \vdots \\ x_{n1} & x_{n2} & \cdots & x_{np} \end{bmatrix}. \tag{5}$$

Establish the correlation coefficient matrix R of variables and find the characteristic root of R ($\lambda_1 \geq \lambda_2 \geq \cdots \lambda_p > 0$) and its corresponding unit characteristic vector $(e_1, e_2, \cdots, e_p)$.

Then, determine the number of principal components, define the contribution rate of the principal components which is $\lambda_i / \sum_{k=1}^{p} \lambda_k$, $(i = 1, 2, \cdots, p)$, and the cumulative contribution rate is $\sum_{k=1}^{i} \lambda_k / \sum_{k=1}^{p} \lambda_k$, $(i = 1, 2, \cdots, p)$.

Generally, the eigenvalues $\lambda_1, \lambda_2, \cdots \lambda_m$ corresponding to the first, second, ..., mth $(m \leq p)$ principal components whose cumulative contribution rate reaches 85% or more are taken. The PCA model can be formulated as

$$\begin{cases} f_1 = e_{11}x_1 + e_{12}x_2 + e_{13}x_3 + \cdots + e_{1p}x_p, \\ f_2 = e_{21}x_1 + e_{22}x_2 + e_{23}x_3 + \cdots + e_{2p}x_p, \\ \vdots \\ f_m = e_{m1}x_1 + e_{m2}x_2 + e_{m3}x_3 + \cdots + e_{mp}x_p, \end{cases} \tag{6}$$

where e_{ip} is the p-dimensional eigenvector corresponding to the i-th eigenvalue of the correlation matrix of the original variables; $[x_1\ x_2 \cdots x_p]^T$ is the p-dimensional initial input variable.

Principal component analysis was performed on the characteristic parameters of the oil-water two-phase ultrasonic power spectrum, and the results are shown in Table 2.

It can be seen from Table 2 that the cumulative contribution rate of the first component reaches 86.087%, which exceeds 85%, which can well summarize the original variables. Therefore, the principal component of the characteristic parameters of the oil-water two-phase ultrasonic power spectrum is the first extracted. According to the component score coefficient matrix, the expression can be obtained as

$$F_1 = 0.163X_1 - 0.146X_2 + 0.162X_3 - 0.155X_4 - 0.144X_5 + 0.148X_6 + 0.159X_7. \tag{7}$$

Table 3: Approximate value matrix table of related variables for oil-water two-phase flow.

	Correlation between vectors of power spectrum								
	Total flow	Water cut	Peak amplitude	Center frequency	Amplitude of oil	Frequency of oil	Variance of oil	Area of oil peak	Amplitude ratio
Total flow	1.000	.000	.667	-.555	.668	-.573	-.455	.651	.659
Water cut	.000	1.000	-.651	.601	-.648	.656	.556	-.647	-.690
Peak amplitude	.667	-.651	1.000	-.778	.999	-.852	-.807	.939	.975
Center frequency	-.555	.601	-.778	1.000	-.766	.959	.853	-.630	-.719
Amplitude of oil	.668	-.648	.999	-.766	1.000	-.837	-.790	.947	.979
Frequency of oil	-.573	.656	-.852	.959	-.837	1.000	.933	-.687	-.784
Variance of oil	-.455	.556	-.807	.853	-.790	.933	1.000	-.572	-.684
Area of oil peak	.651	-.647	.939	-.630	.947	-.687	-.572	1.000	.983
Amplitude ratio	.659	-.690	.975	-.719	.979	-.784	-.684	.983	1.000

Table 4: Results of PCA for water cut.

Component	Eigenvalue	Variance contribution rate/%	Cumulative variance contribution rate/%
1	6.09	87.002	87.002
2	0.675	9.639	96.641
3	0.18	2.565	99.207
4	0.035	0.502	99.709
5	0.013	0.19	99.899
6	0.005	0.072	99.971
7	0.002	0.029	100

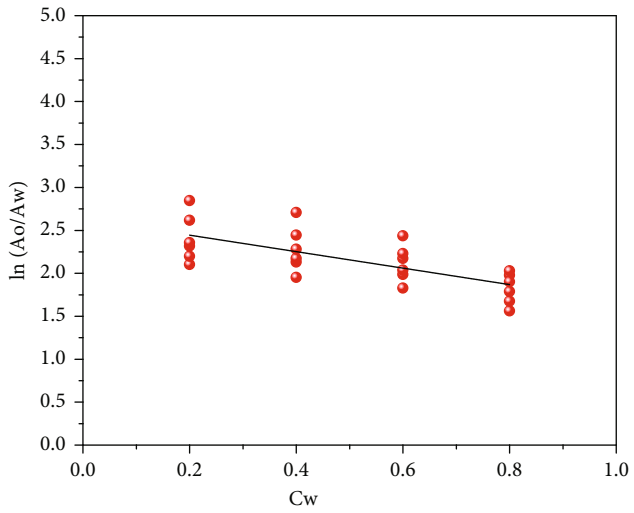

Figure 8: Intersection diagram of water cut and amplitude ratio.

Therefore, the oil flow rate and the principal components extracted from the characteristic parameters of the ultrasonic power spectrum are used for the rendezvous analysis to predict the oil flow rate. The result is shown in Figure 6.

Figure 6 is fitted to get the relationship between the oil flow rate (Q_o) and the principal component value (F_1) measurement model which is

$$Q_o = 7.5778F_1 + 11.667. \tag{8}$$

The oil flow rate increases linearly with the principal component value, and it has very good monotonicity. When the oil flow rate is small, the data correlation is obviously stronger than when the oil flow rate is high, indicating that the ultrasonic flow logging tool is more sensitive to small oil flow changes under the conditions of low oil flow and high water holdup. This is because when the oil flow is low and the wellbore water holdup is high, the size and number of oil bubbles are small, and the oil phase is evenly distributed, which is conducive to ultrasonic Doppler measurement. When the oil flow rate increases and water holdup decreases, the size and number of oil bubbles in the wellbore increase, small oil bubble collision and aggregation become larger, oil phase distribution is uneven, ultrasonic Doppler measurement sensitivity decreases, reflection intensity increases, and amplitude increases. Therefore, ultrasonic Doppler measurement has high sensitivity to high water cut.

Substituting the data obtained from the ultrasonic measurement experiment of the oil-water two-phase flow into Eq. (8), the oil flow rate prediction results as shown in Figure 7 is obtained. In the case of different total flow, the oil flow value in the ultrasonic multiphase flow simulation experiment is in good agreement with the oil flow prediction value.

Table 5: Analysis table of partial correlation of variables related to oil-water two-phase flow.

Correlation Control variable			Water cut	Amplitude of oil	Frequency of oil	Area of oil peak	Amplitude ratio
Total flow	Water cut	Correlation	1.000	-.872	.800	-.852	-.918
		Significance (two-tailed)	.	.000	.000	.000	.000
		Degree of freedom	0	21	21	21	21
	Amplitude of oil	Correlation	-.872	1.000	-.745	.907	.963
		Significance (two-tailed)	.000	.	.000	.000	.000
		Degree of freedom	21	0	21	21	21
	Frequency of oil	Correlation	.800	-.745	1.000	-.505	-.660
		Significance (two-tailed)	.000	.000	.	.014	.001
		Degree of freedom	21	21	0	21	21
	Area of oil peak	Correlation	-.852	.907	-.505	1.000	.971
		Significance (two-tailed)	.000	.000	.014	.	.000
		Degree of freedom	21	21	21	0	21
	Amplitude ratio	Correlation	-.918	.963	-.660	.971	1.000
		Significance (two-tailed)	.000	.000	.001	.000	.
		Degree of freedom	21	21	21	21	0

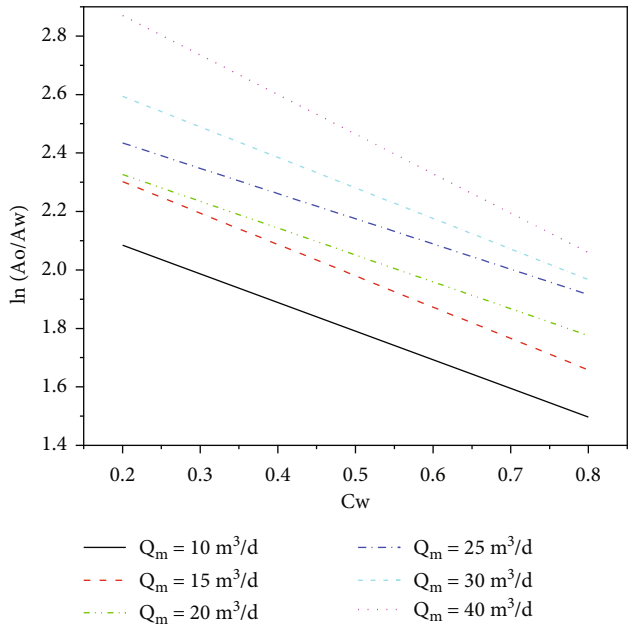

Figure 9: The relationship between water cut and amplitude ratio at the same total flow rate.

On the whole, the oil flow rate prediction model established by the hydrostatic oil injection experiment data is effective in calculating the oil flow rate under the oil-water two-phase flow. The overall average absolute error is 0.92 m^3/d, and the average relative error is 10.36%.

Although the oil flow rate in oil-water two-phase flow can be accurately calculated by extracting principal component value of the characteristic parameters of the ultrasonic power spectrum, the main reason is that the total flow rate is small, the oil phase velocity is close to the static drift velocity of oil in water, and the change of oil flow rate mainly depends on the number of oil bubbles (oil holdup), which is strongly related to the amplitude of oil and area of oil peak. The total flow does not change, the water cut decreases, and as the oil flow increases, the error value increases. That is to say, the prediction model (8) has higher prediction accuracy in the case of high water cut and less oil bubbles. With the increase of oil bubbles, the flow pattern changes from discrete bubble flow to emulsion flow, and the measurement effect becomes worse.

3.3. Water Cut Measurement and Description of the Algorithm. In the previous section, it was shown that the PDF and PSD of the differential ultrasonic power spectrum characteristic parameters followed certain systematic trends as the oil, and water flow rates were changed [29].

The water cut reflects the relationship between the water flow and the total flow in the oil-water two-phase flow and has a complicated relationship with factors such as water holdup and oil-water slip velocity. In the oil-water two-phase flow of low-yield liquid, the water holdup is generally high due to the serious water logging in the wellbore, which brings more difficulties to the calculation of water cut. The conventional production profile interpretation model (drift flux model, slip model) is greatly affected by the fluctuation of water holdup. Ultrasonic multiphase flow logging data processing uses the power spectrum related characteristic parameters to compare and analyze the water cut ratio of the experiment to determine the water cut calculation model. In the same way, for the water prediction, the PDF and PSD are also calculated from the input signal, appropriate features are extracted by using DCA followed by PCA, and regression is performed using artificial neural networks.

It can be seen from the power spectrum analysis of ultrasonic measurement in Figures 4 and 5 that the total flow rate has no obvious dependence on the related characteristic parameters, when the total flow rate remains unchanged, the water cut increases, the amplitude of the corresponding

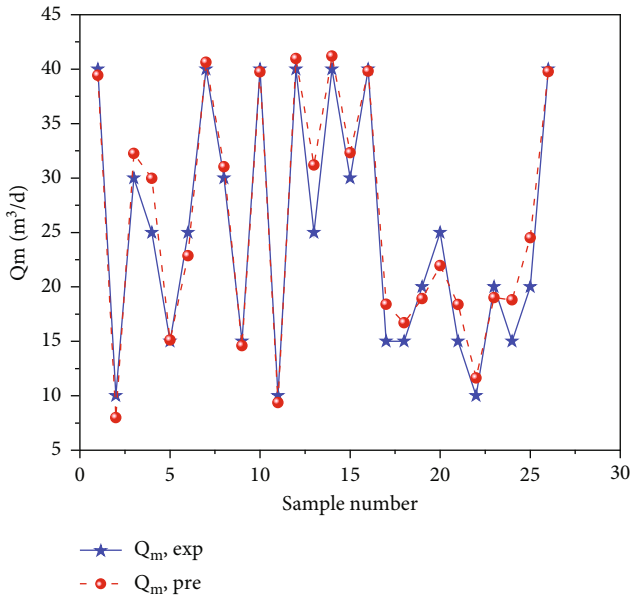

Figure 10: Comparison chart of predicted flow and real flow.

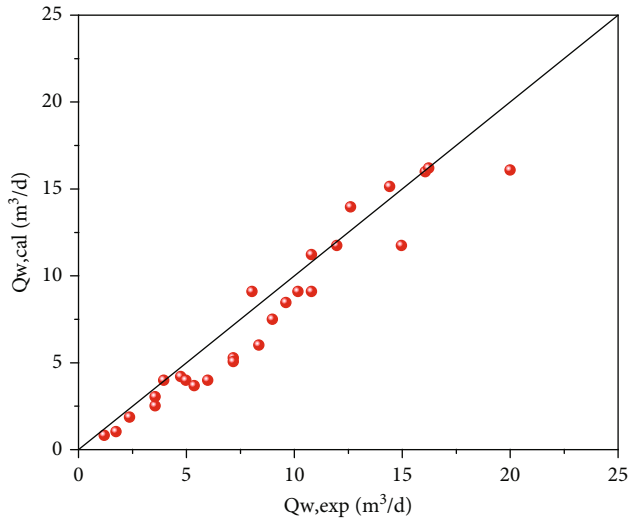

Figure 11: Comparison diagram of experimental and calculated water phase flow.

power spectrum decreases, and the center frequency shifts to the right. Therefore, the distance correlation analysis (DCA) method is also used to perform correlation analysis on the experimental data of the oil-water two-phase flow. The analysis results are shown in Table 3. According to the analysis results, Pearson correlation coefficients between total flow and amplitude peak, center frequency, amplitude of oil, frequency of oil, variance of oil, area of oil peak, and amplitude ratio are not high, all less than 0.7, indicating that the distance correlation intensity between them is very weak, which is consistent with the qualitative analysis results of power spectrum in Figures 4 and 5.

The Pearson correlation coefficient between water cut and ultrasonic characteristic parameters is not high, which

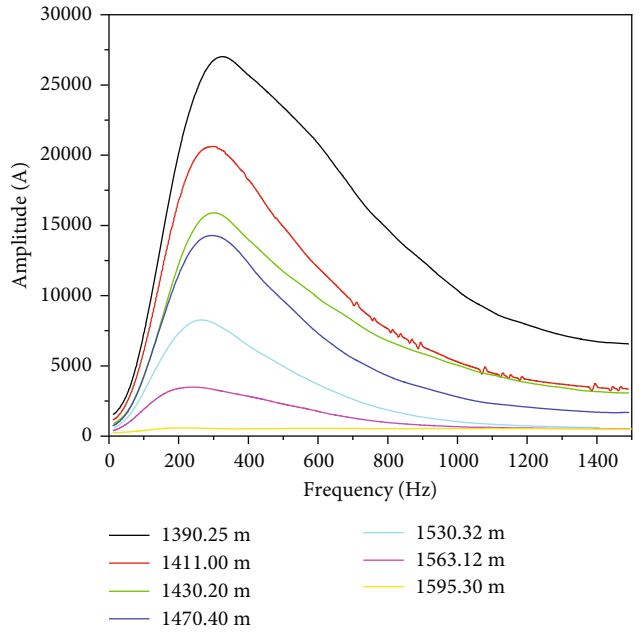

Figure 12: Well 13-1-2 ultrasonic multiphase flow test power spectrum curve.

is positively correlated with the center frequency, frequency of oil and variance of oil, but negatively correlated with the amplitude peak, amplitude of oil, area of oil peak, and amplitude ratio. Pearson correlation coefficient with the total flow is 0, and there is no correlation between water cut and the total flow. In the case of oil-water two-phase flow, the peak amplitude is positively correlated with the oil amplitude, and the center frequency is positively correlated with the frequency of oil. The correlation coefficient is relatively close, and the correlation coefficient with the oil-water amplitude ratio ($\ln\ (A_o/A_w)$) is 0.69.

To investigate the effect of representing the total information in the original dataset with a smaller number of features, principal component analysis was performed on the characteristic parameters of the oil-water two-phase ultrasonic power spectrum, and the results are shown in Table 4.

According to the component score coefficient matrix, the expression can be obtained as

$$F_2 = 0.158X_1 - 0.149X_2 + 0.163X_3 - 0.156X_4 - 0.144X_5 + 0.143X_6 + 0.158X_7. \quad (9)$$

Figure 8 is the intersection of the water cut and the oil-water amplitude ratio, and the fitting formula is Eq. (10):

$$\mathrm{Ln}\left(\frac{A_o}{A_w}\right) = 0.098974C_w + 2.60833. \quad (10)$$

The linear fitting correlation coefficient ($R^2 = 0.45784$) is low, and the water cut calculated by Eq. (10) has a large error, which can be used as the pseudowater cut calculation formula.

Table 6: Well 13-1-2 power spectrum characteristic parameter table.

Layer number	Measuring point depth (m)	Temperature (°C)	Pressure (MPa)	Peak amplitude (μv/Hz^2)	Center frequency (Hz)	Amplitude of oil (μv/Hz^2)	Frequency of oil (Hz)	Fluid phase
1	1390.25	68.00	2.90	1067.00	326.34	812.51	361.70	Oil-water two-phase
2	1411.00	68.80	3.10	812.53	297.02	636.01	322.33	Oil-water two-phase
3	1430.20	69.80	3.30	623.64	301.73	469.24	326.78	Oil-water two-phase
4	1470.40	71.40	3.80	559.80	295.98	453.81	314.15	Oil-water two-phase
5	1530.32	73.50	4.40	314.81	268.70	236.23	261.76	Oil-water two-phase
6	1563.12	74.50	4.80	129.34	241.65	106.64	283.13	Oil-water two-phase
7	1595.30	76.64	5.14	13.46	221.14	0.00	0.00	Static water

Further analysis of moisture content and the relationship between ultrasonic power spectrum parameters, extraction, and analysis of the results of correlation coefficient absolute value are greater than 0.6 variable frequency amplitude (amplitude of oil, frequency of oil, area of oil peak, amplitude ratio), the partial correlation analysis (PCA) method, analysis of traffic is fixed, and the water cut and the correlation between ultrasonic power spectral characteristic parameters process the results as shown in Table 5. It can be seen from the results that when controlling the total flow, the partial correlation coefficient between the water cut and the amplitude ratio is -0.918, and the probability (significance) that they are not correlated is $p = 0$. It can be concluded that under the condition of a certain total flow, there is a significant negative correlation between water cut (C_w) and oil-water amplitude ratio ($\ln(A_o/A_w)$). Figure 9 is a graph showing the relationship between water cut and amplitude ratio when the total flow rate is constant under the oil-water two-phase flow.

It can be seen from Figure 9 that under a certain total flow rate, the water cut and the oil-water amplitude ratio have a good linear correlation. The larger the amplitude ratio, the smaller the water cut. Using this chart, you can calculate the water cut based on the amplitude ratio interpolation when the total flow rate is determined, and you can also calculate the total flow rate based on the amplitude ratio interpolation when the water cut rate is determined. For the flow rate prediction, water cut (C_w) and oil-water amplitude ratio ($\ln(A_o/A_w)$) were used as inputs to multilayer back-propagation neural networks, which gave the total flow rates as output. Figure 10 presents the ratio of predicted and measured flow rates for the ANN; the vast majority of predictions were within ±10% of the measured values.

3.4. Water Phase Flow Calculation. From the above power spectrum Figure 5 and the distances process correlation analysis result Table 3, it can be seen that it is difficult to directly find the relationship between the water phase flow rate and the relevant characteristic parameters of the power spectrum. However, under a certain total flow rate, the relationship between the ratio of the water phase flow rate and the amplitude obtained from the water cut is very obvious, and the linear relationship is better. Therefore, based on the above Eq. (5) of the oil phase flow calculation model and the water cut calculation chart under a certain total flow, the following method is proposed to calculate the water phase flow.

(1) First, calculate the oil phase flow rate Q_o from the principal component value (F_1) using Eq. (8)

(2) From the oil-water amplitude ratio (ln (Ao/Aw)), use Eq. (9) to calculate the pseudo water cut C_w'

(3) Then, use the oil-water amplitude ratio (ln (Ao/Aw)) and the pseudowater cut C_w' obtained in step (2) into the same water cut and amplitude ratio relationship chart (Figure 9) for the total flow rate for ANN to obtain the total flow rate Q_m. Recalculate the water cut according to the definition formula of water cut

$$C_w = \frac{Q_m - Q_o}{Q_m}. \tag{11}$$

(4) Then calculate the error between the water cut calculated by Eq. (7) and the pseudowater cut calculated by Eq. (6). If it is within the error range, the total flow Q_m and water cut C_w can be obtained, and the water phase flow can be calculated by the relationship between them

$$Q_w = Q_m \cdot C_w. \tag{12}$$

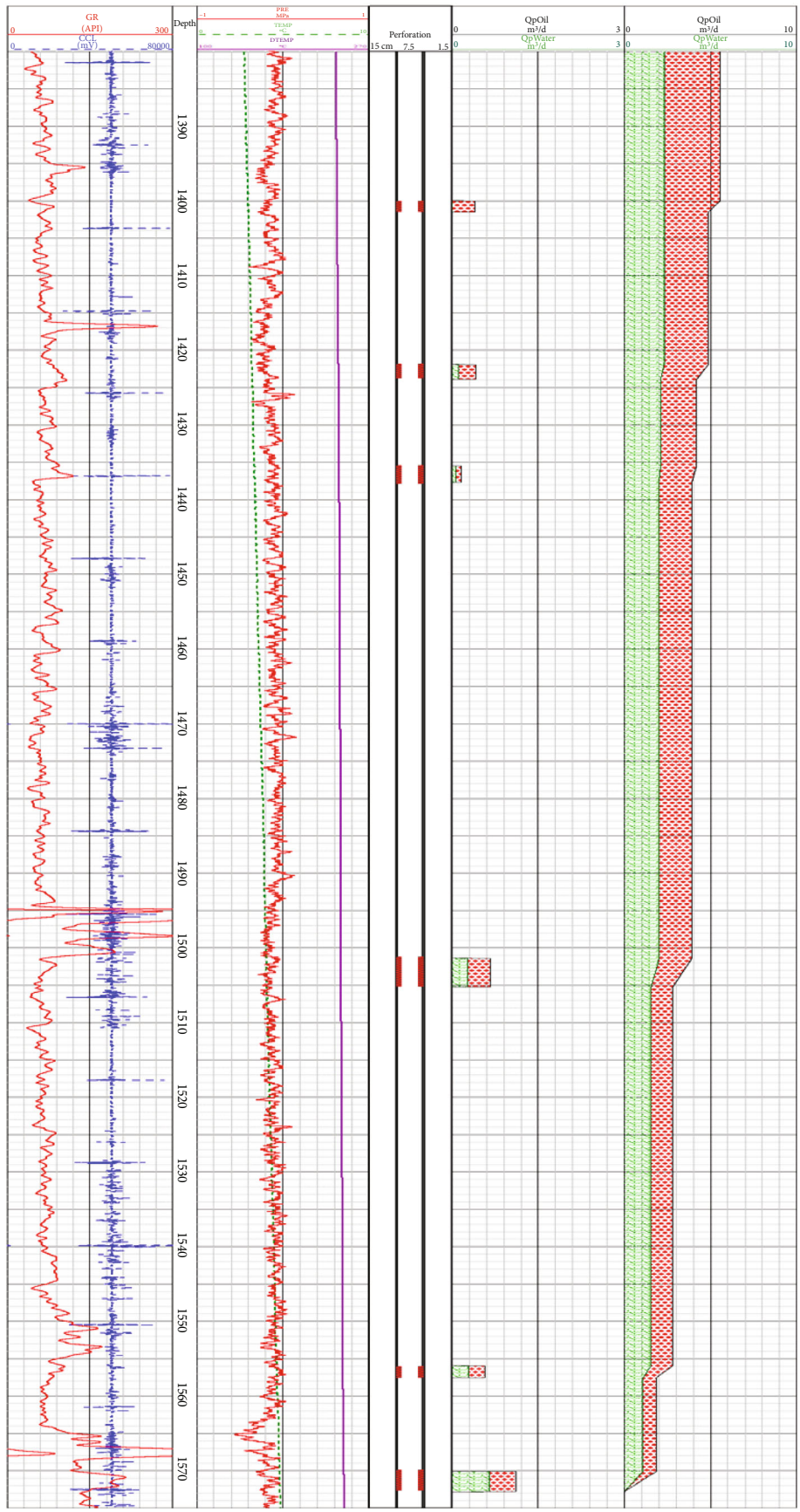

Figure 13: Interpretation results of well 13-1-2.

Table 7: Well 13-1-2 interpretation result table.

Serial number	Interpretation level	Perforated well section (m)	Oil yield (m^3/d)	Water yield (m^3/d)	Total fluid production (m^3/d)	Water cut (%)
1	IV-25	1400.00-1401.50	0.68	0	0.68	0
2	IV-28	1421.90-1423.90	0.5	0.19	0.69	27.09
3	IV-30	1435.47-1437.70	0.17	0.1	0.27	36.98
4	IV-40	1501.38-1505.22	0.65	0.46	1.11	41.64
5	IV-47	1555.95-1557.55	0.49	0.48	0.97	49.42
6	IV-49	1570.10-1572.80	0.77	1.07	1.84	58.36
Total			3.26	2.3	5.56	41.37

(5) If the error is greater than the error limit, adjust the pseudowater cut C_w' according to the relationship between the water cut C_w calculated on the plate and the pseudowater cut C_w' and continue to insert it into the Figure 9 for interpolation calculations until the error is less than the error limit

In order to check the calculation accuracy of the method, the logging data of the ultrasonic Doppler flowmeter in the full flow layer of 26 wells were measured by power spectrum processing to extract the relevant characteristic parameters. Because the calibration conditions of the logging instrument laboratory are different from the working conditions of downhole logging, and the physical properties of oil and water are different, it is necessary to calibrate the amplitude and center frequency of the total flow power spectrum curve of the downhole test to the calibration conditions of the same flow rate for explanation [4]. The calibration coefficient is

$$\begin{cases} K_A = A_{\log}/A_{\exp}, \\ K_F = F_{\log}/F_{\exp}. \end{cases} \tag{13}$$

In the formula, K_A is the amplitude correction coefficient, $A_{\log}$ is the actual logging amplitude value, $A_{\exp}$ is the amplitude value measured in the laboratory with the same flow rate, K_F is the frequency correction coefficient, $K_{\log}$ is the actual logging frequency value, and $K_{\exp}$ is the frequency value measured by the laboratory with the same flow rate.

The calibrated power spectrum characteristic parameter values were substituted into the above formula and chart, and the interpretation results were compared with the water flow calculated by the total production and water cut of logging time at that time. The comparison between the actual water flow in the full flow layer of these 26 wells and the water flow calculated by this method is shown in Figure 11. The average absolute error of the water phase flow calculation is 1.502 m^3/d, and the average relative error is 22.79%. The relative error of the water phase flow rate under high water cut conditions is obviously smaller than the relative error value under low water cut conditions, which also shows that the ultrasonic Doppler oil-water two-phase flow measurement has higher sensitivity under high water cut conditions.

4. Field Application

Western Oilfield is a low-porosity and low-permeability reservoir. It is currently in the middle and late stages of development, and most of the oil wells are in a state of low production fluid and high water cut. Well 13-1-2 is a pumped well. Ultrasonic multiphase flow production profile logging was performed on March 23, 2018. Before logging, the daily production fluid at the wellhead was 5.55 m^3/d, and the water cut was 41.4%.

The logging interpretation of ultrasonic polyphase abortion profile is mainly based on the temperature, pressure, and power spectrum curve of downhole fluid to judge the phase state of downhole fluid, and the oil and water production of each producing zone is calculated according to the production status of wellhead and the amplitude and central frequency of oil signal of power spectrum curve. The power spectrum curve of ultrasonic multiphase flow test in well 13-1-2 is shown in Figure 12.

According to the position of the downhole perforation layer, there are a total of 7 test points, and the test point fluid is a two-phase flow of oil and water. The power spectrum curve of each test point is processed to obtain the power spectrum characteristic parameters, as shown in Table 6.

The comprehensive interpretation results are shown in Figure 13, and the interpretation results are shown in Table 7. After comprehensive analysis, the interpretation results are obtained: the main liquid producing layer is IV-49 sublayer, the liquid production volume is 1.84 m^3/d, and the water cut is 58.36%. The secondary liquid producing layers are IV-25, IV-28, IV-30, IV-40, and IV-47, with liquid production of 0.68 m^3/d, 0.69 m^3/d, 0.27 m^3/d, 1.11 m^3/d, and 0.97 m^3/d, respectively. Water cut were 0.0%, 27.09%, 36.98%, 41.64%, and 49.42%, respectively.

Compared with the actual oil and water flow in the field, the accuracy of data-driven artificial intelligence interpretation is higher than that of traditional ultrasonic power spectrum single-factor calculation of flow, and it also solves the problem of water flow calculation.

5. Conclusion

In this paper, the ultrasonic multiphase flow logging tool is used to test the acoustic frequency characteristics of the oil-water two-phase flow in a vertical simulation experimental wellbore, and the data-driven methodology is used for the

prediction of fluid flow in ultrasonic production logging data processing. The following conclusions are obtained through the analysis of the experimental data.

(1) The ultrasonic multiphase flow logging tool mainly detects the movement parameters of the oil bubbles in the continuous water phase. The power spectrum curve obtained from the experimental data can qualitatively analyze the change characteristics of the total flow rate and water cut of the oil-water two-phase flow

(2) Under low flow conditions, the oil bubbles move upward at a static drift speed; so, the oil phase flow is mainly related to the number of oil bubbles and the ultrasonic reflection intensity that reflects the number of oil bubbles

(3) The characteristic parameters extracted from the ultrasonic power spectrum curve are related to the oil flow and water cut, and there is a functional relationship. This paper uses the distance process correlation analysis method and partial correlation analysis method to analyze the correlation of the power spectrum characteristic parameters and establishes the oil phase flow calculation model, the water cut prediction chart, and the water flow calculation method. The research results show that the method has high precision and can be a very good calculating the output profile parameters of oil-water two-phase flow

(4) The data-driven artificial intelligence interpretation accuracy is higher than the traditional single-factor calculation accuracy of ultrasonic power spectrum

Data Availability

Data is available on request. Please contact the corresponding author for the underlying data supporting the results of the research.

Conflicts of Interest

All authors confirm that there is no financial/personal interest or belief that could affect our objectivity, and no conflicts exist.

Acknowledgments

This research was supported by the National Natural Science Foundation of China (42174155).

References

[1] H. W. Song, H. M. Guo, S. Guo, H. Y. Shi et al., "Measurement method of split-phase flow of oil-water two-phase stratified flow in horizontal wells," *Petroleum Exploration & Development*, vol. 47, no. 3, pp. 573–582, 2020.

[2] A. Zhao, Y. F. Han, Y. Y. Ren, L. S. Zhai, and N. D. Jin, "Ultrasonic method for measuring water holdup of low velocity and high-water-cut oil-water two-phase flow," *Applied Geophysics*, vol. 13, no. 1, pp. 179–193, 2016.

[3] H. Zhuang, *Research on downhole ultrasonic testing method of multiphase flow split flow*, Daqing Petroleum Institute, 2007.

[4] H. Zhang, J. Q. Qiu, Q. C. Wang, C. J. Gan, Y. X. Liu, F. Zhou et al., "Ultrasonic-Doppler three-phase flow logging and its application in Qinghai oilfield," *Logging Technology*, vol. 4, pp. 99–105, 2016.

[5] Q. Wang, X. K. Zheng, F. Y. Meng et al., "Ultrasonic Doppler multiphase flow logging interpretation method based on data mining," *Daqing Petroleum Geology and Development*, vol. 37, no. 6, pp. 149–153, 2018.

[6] E. Abro, V. A. Khoryakov, G. A. Johansen, and L. Kochach, "Improved void fraction determination by means of multibeam gamma-ray attenuation measurements," *Measurement Science and Technology*, vol. 10, no. 2, pp. 99–108, 1999.

[7] M. R. Malayeri, H. Müller-Steinhagen, and J. M. Smith, "Neural network analysis of void fraction in air/water two-phase flows at elevated temperatures," *Chemical Engineering and Processing: Process Intensification*, vol. 42, no. 8-9, pp. 587–597, 2003.

[8] A. Á. D. Castillo, E. Santoyo, and O. Garcia-Valladare, "*A* new void fraction correlation inferred from artificial neural networks for modeling two-phase flows in geothermal wells," *Computational Geosciences*, vol. 41, pp. 25–39, 2012.

[9] S. S. Sablani, W. H. Shayyab, and A. Kacimovc, "Explicit calculation of the friction factor in pipeline flow of Bingham plastic fluids: a neural network approach," *Chemical Engineering Science*, vol. 58, no. 1, pp. 99–106, 2003.

[10] B. Goutorbe, F. Lucazeau, and A. Bonneville, "Using neural networks to predict thermal conductivity from geophysical well logs," *Geophysical Journal International*, vol. 166, no. 1, pp. 115–125, 2006.

[11] A. Bassam, D. Ortega-Toledo, J. A. Hernández, J. G. González-Rodriguez, and J. Uruchurtu, "Artificial neural network for the evaluation of CO 2 corrosion in a pipeline steel," *Journal of Solid State Electrochemistry*, vol. 13, no. 5, pp. 773–780, 2009.

[12] E. A. Osman, "Artificial neural networks models for identifying flow regimes and predicting liquid holdup in horizontal multiphase flow," in *Proceedings of the SPE Middle East Oil and Gas Show and Conference*, Manama, Bahrain, 2001.

[13] X. Zhao, N. D. Jin, and W. Li, "Soft measurement method of phase volume fraction for oil/water two-phase flow," *Journal of Chemical Industry and Engineering (China)*, vol. 56, pp. 1875–1879, 2005.

[14] R. Silva and P. Melo-Pinto, "A review of different dimensionality reduction methods for the prediction of sugar content from hyperspectral images of wine grape berries," *Applied Soft Computing*, vol. 113, article 107889, 2021.

[15] K. Pearson, "LIII.On lines and planes of closest fit to systems of points in space," *The London, Edinburgh, and Dublin philosophical magazine and journal of science*, vol. 2, no. 11, pp. 559–572, 1901.

[16] H. Hotelling, "Analysis of a complex of statistical variables into principal components," *Journal of Education & Psychology*, vol. 24, no. 6, pp. 417–441, 1933.

[17] S. Deegalla, H. Boström, and K. Walgama, "Choice of dimensionality reduction methods for feature and classifier fusion with nearest neighbor classifiers," in *15th International Conference on Information Fusion (FUSION)*, pp. 875–881, Singapore, 2012.

[18] S. Ahmadkhani and P. Adibi, "Face recognition using supervised probabilistic principal component analysis mixture model in dimensionality reduction without loss framework," *IET Computer Vision*, vol. 10, no. 3, pp. 193–201, 2016.

[19] C. Meng, O. A. Zeleznik, G. G. Thallinger, B. Kuster, A. M. Gholami, and A. C. Culhane, "Dimension reduction techniques for the integrative analysis of multi-omics data," *Briefings in Bioinformatics*, vol. 17, no. 4, pp. 628–641, 2016.

[20] I. T. Jolliffe and J. Cadima, "Principal component analysis: a review and recent developments," *Philosophical Transactions of the Royal Society A: Mathematical, Physical and Engineering Sciences*, vol. 374, no. 2065, article 20150202, 2016.

[21] D. W. Baker and W. G. Yates, "Technique for studying the sample volume of ultrasonic Doppler devices," *Medical and Biological Engineering*, vol. 11, no. 6, pp. 766–770, 1973.

[22] C. Tan, M. Yuichi, W. L. Liu, T. Yuji, F. Dong, and T. Yasushi, "Ultrasonic Doppler technique for application to multiphase flows: a review," *International Journal of Multiphase Flow*, vol. 144, no. 2021, article 103811, 2021.

[23] Z. H. Li, L. B. Liu, T. S. Jiang, H. M. Duan, X. Z. Zhai et al., "The spectral characteristics of the ultrasonic Doppler signal in flow measurement and its relationship with the flow velocity in the pipeline," *Acta Metrology*, vol. 16, no. 1, pp. 68–72, 1995.

[24] W. J. Yang, W. Z. Chen, Q. F. Zhao, Z. G. Jiang et al., "Multiphase flow ultrasonic logging simulation experiment research," *Journal of Jianghan Petroleum Institute*, vol. 4, pp. 76-77, 2003.

[25] X. P. Liu, X. Wang, Y. Liu, J. C. Chen, X. Q. Li et al., "Research on slip ratio correction method of water cut and its application in Zhongyuan oilfield," *Fault Block Oil and Gas Field*, vol. 5, pp. 66-67, 2003.

[26] N. D. Jin, W. K. Ren, X. Chen, L. S. Zhai et al., "Gas holdup measurement of oil-gas-water three-phase flow ultrasonic sensor," *Journal of Applied Acoustics*, vol. 39, no. 1, pp. 36–44, 2020.

[27] X. Longhan and S. Tao, *SPSS statistical analysis and data mining*, Publishing House of Electronics Industry, 2012.

[28] Z. Zhihua, *Machine Learning*, Tsinghua University Press, Beijing, 2016.

[29] H. Shaban and S. Tavoularis, "Measurement of gas and liquid flow rates in two-phase pipe flows by the application of machine learning techniques to differential pressure signals," *International Journal of Multiphase Flow*, vol. 67, pp. 106–117, 2014.